

# A Therapist-taught Robotic System for Assistance During Gait Therapy Targeting Foot Drop

Jason Fong<sup>1</sup>, Hossein Rouhani<sup>2</sup>, and Mahdi Tavakoli<sup>1</sup>

**Abstract**—The adoption of robots in rehabilitation medicine settings has become increasingly attractive in recent years. Robots are capable of providing repetitive, high-intensity physiotherapy. In this paper, we apply kinesthetic teaching principles to a robotic system in order to allow it to first learn and then imitate a therapist’s behavior when assisting a patient in a lower limb therapy task. A therapist’s assistance in lifting a patient during treadmill-based gait therapy is statistically encoded by the system using Learning from Demonstration (LfD) techniques. Later, the therapist’s assistance is imitated by the robot, allowing the patient to continue practicing in the absence of the therapist. Preliminary experiments are performed with inexperienced users playing the role of the assisting therapist, and with healthy participants (wearing an elastic cord to simulate foot drop) playing the role of the patient. Toe clearance values are recorded and show that the system is able to provide the full clearance needed by the patient to practice in the absence of the therapist.

**Index Terms**—Rehabilitation Robotics; Physical Human-Robot Interaction; Learning from Demonstration

## I. INTRODUCTION

AS the world’s population increases in age, the integration of robotic assistance in rehabilitation medicine settings continues to become more attractive, as well as feasible with innovations in technology. Robots enable the provision of repetitive, high-intensity physiotherapy [1] which is an essential component to post-stroke rehabilitation as an example. Stroke is the fifth leading cause of death globally, causing approximately 6.5 million deaths each year [2], and typically leaving survivors with neuromuscular disability and without the ability to live independently. Post-stroke therapy emphasizes repeated activation and use of a patient’s affected muscles in order to reassociate damaged neural structures and regain muscle tone [3]. Doing so can allow a patient to relearn how to perform activities that are categorized as essential to living, commonly referred to as Activities of Daily Living (ADLs), and thereby regain some degree of independence.

Manuscript received: July, 31, 2018; Revised October, 31, 2018; Accepted December, 2, 2018.

This paper was recommended for publication by Editor Allison Okamura upon evaluation of the Associate Editor and Reviewers’ comments. This work was supported by the Canada Foundation for Innovation (CFI) under grant LOF 28241; the Alberta Innovation and Advanced Education Ministry under Small Equipment Grant RCP-12-021; the Natural Sciences and Engineering Research Council (NSERC) of Canada under the Collaborative Health Research Projects (CHRP) Grant #316170; and the Quanser, Inc.

<sup>1</sup>Jason Fong and Mahdi Tavakoli are with the Department of Electrical and Computer Engineering, University of Alberta, Edmonton, AB, Canada. {jmfong, mahdi.tavakoli}@ualberta.ca

<sup>2</sup>Hossein Rouhani is with the Department of Mechanical Engineering, University of Alberta, Edmonton, AB, Canada. hrouhani@ualberta.ca  
Digital Object Identifier (DOI): see top of this page.

ADLs are often difficult to perform for stroke survivors because of their lack of muscular coordination and muscle weakness. Hemiparesis, in particular, is common to stroke survivors, in which the decrease in muscular coordination and tone present themselves on one side of the survivor’s body. ADLs can typically be divided into those that demand the use of a patient’s upper limbs, such as cooking or grooming, and those that involve their lower limbs, such as walking, sitting, or standing. In performing lower limb ADLs, the difficulty experienced by hemiparetic patients can lead to the development of compensatory strategies, which may result in undesirable and unsafe walking patterns, sitting, and standing transfers, or in extreme cases the neglect of their affected side [4], [5]. As a result, specific physiotherapy routines are designed in order to assist patients in relearning and reinforcing correct gait habits.

Body weight supported treadmill training (commonly referred to as BWSTT) is one such routine. BWSTT involves the suspension of a patient using a harnessing device above a treadmill, such that a portion of their body weight is relieved. If the patient is ambulatory, this allows them to practice walking without needing the full muscle coordination and tone normally involved. If the patient is non-ambulatory, typically 2-3 therapists will be present during therapy and will physically hold and move the patient’s lower limbs through a proper walking pattern, allowing the patient to experience walking. In non-ambulatory patients, in particular, BWSTT has been shown to provide greater improvements to participants’ gait than traditional lower limb physiotherapy, which consists of simple muscle strengthening exercises [6]–[8].

However, the physical exertion required by therapists in the case of non-ambulatory patients is very intensive; therapy sessions are often limited to 15-20 minutes and with only one session per day [9]. Numerous robotic solutions have been proposed in the past decade in an effort to alleviate this physical burden [7], [10]–[12]. These technologies typically take the form of exoskeletons, treadmill or footplate-integrated robots, powered orthoses, or functional electric stimulators (FES).

Robotic lower-limb assistive devices have traditionally been programmed to assist the user in following predefined trajectories (i.e., gait patterns) with minimal allowed deviation [13]. This is less than ideal, as patients often feel like they are fighting the robotic assistance, should their desired movements not match with the assistance provided [14]. More recently, adaptive control schemes have received a large amount of attention. Lower-limb exoskeletons and ankle-foot orthoses, in particular, have had a significant number of such strategies developed for them. [15] utilizes adaptive oscillators as Central

Pattern Generators (CPG) in order to provide natural gait patterns through learned motor primitives, while [16] applies a similar concept based on using EEG measurements as input to a CPG. [17], [18] incorporate force-feedback reflex-based neuromuscular models. [19] uses complementary limb motion estimation to provide assistance to the affected lower-limb that mimics the motion of a user's healthy limb. [20], [21] implement variable-impedance controlled systems, based on different measurements of the user's performance. However, one common issue with these systems is that the role of a supervising therapist is limited. At most, their role is to provide the exoskeleton with trajectories of ideal gait (in the case of motor primitives), after which variation of the assistance level is fully up to the adaptive algorithm. This is typically undesirable for therapists, as the idea of robotic automation with minimal input from clinicians is poorly received [22]. Another possible form of adaptation we propose would be to allow the therapist to provide and modify behaviors (for the robot to imitate) as they see fit, where the behaviors do not have to be ideal but could be the most appropriate for a patient's capabilities. In this manner, the therapist stays involved in therapy as much as possible while the robot alleviates only the burdensome physical aspects.

The application of machine learning techniques to enable this adaptation across robotic rehabilitation has gained increasing interest in recent years. In upper limb rehabilitation, several uses of this same paradigm have been explored [23]–[26]. The inclusion of machine learning in lower limb robotic assistance has received attention mainly on recognizing gait cycle movement patterns [27], [28], but less on learning the correct corresponding assistance dependent on these patterns. A method of providing therapists with finer control for tuning the amount of assistance provided to patients during gait therapy instead of using predefined fixed assistance regimes observed in traditional assistive robotics is thus examined.

The contribution of this paper is to propose a proof-of-concept treadmill-based gait therapy system that utilizes machine learning techniques to allow a therapist to intuitively define the amount of assistance provided to a patient and to allow a robot to learn and later reproduce the same assistance in the absence of the therapist. This is done through the use of Learning from Demonstration (LfD) techniques, where a user typically physically holds and moves a robot along a trajectory which the robot learns and is later able to imitate. The system learns by observing and generalizing between multiple demonstrations from a therapist, as opposed to following a single desired trajectory. Additionally, this method is advantageous for use in clinical settings, as the therapists can train the system without having to possess computer programming know-how. To our knowledge, this is the first application of this paradigm to the study of lower limb rehabilitation.

We draw inspiration from the design of the KineAssist, a robotic treadmill-based assistive device that operates only in one degree of freedom (DOF) [29]. The KineAssist consists of a harness that holds the patient, attached to a vertical linear rail at the back of a treadmill. Force sensors on the device allow a therapist to provide lifting assistance to the patient during parts of ADLs or the gait cycle that require compensation for the

patient's disability. This design maximizes patient participation while maintaining patient stability in order to prevent falls, but lacks machine learning capabilities. Our system is based on a robot manipulator (i.e., industrial robot) available to us, instead of a mechanized rail, as in the case of the KineAssist, or a wearable robot, as in the case of most gait therapy solutions. The robot will provide lifting assistance to the user representing the patient through a rope and pulley system that will hoist the harnessed participant in one DOF (in the vertical axis); the exact setup will be discussed later. Foot drop is a commonly observed pathology in stroke survivors which we focus on in this work. Toe clearance during the swing phase of the affected limb is a major difficulty experienced by patients with foot drop [30]. Our objective is to learn and train the system to provide an adequate amount of lifting assistance so as to provide the minimal toe clearance for the patient to be able to practice walking by themselves and more specifically the dorsiflexion of their affected foot. We will examine if the trained system can assist the affected limb in such a way that its toe clearance matches that of the unaffected foot during assistance as well as the toe clearance values of both feet of a healthy individual.

The paper is structured as follows: Section II outlines the approaches to LfD and human-robot interaction (HRI) incorporated into this work, Section III describes the experimental setup and presents results, IV provides discussion of the system and its performance, and V provides concluding remarks and future directions for the work.

## II. PROPOSED APPROACH

We aim to produce a robotic system that provides assistance during gait therapy by partially lifting a patient's affected leg during the swing phase of their stride. The robot should learn the amount and timing of assistance to give by first observing a therapist providing assistance to a patient as in during typical BWSTT, i.e., adjusting the trajectories of the patient's foot, knee, or hip. The therapist should provide assistance by physically holding and moving the robot, which is attached to the patient. Due to the nature of this task, we consider the patient's affected foot (and more specifically their toe) position to be the measurable outcome. This means that during the therapist's demonstration, the motion of the patient's foot and the positions the therapist moves the robot to should be recorded and a model generated to relate the two. Then, during the phase where the therapist is no longer present, which we call the imitation phase, the robot should be able to provide similar assistance by partially lifting the patient in a safe and non-disruptive way. We then need two main components to control the robot. First, since the therapist should be able to move the robot by applying force to its end-effector when demonstrating assistance, a robot control scheme designed for safe physical human-robot interaction (PHRI) should be incorporated. The Time Delay Estimation (TDE) impedance control method is selected for this (explained in Section II-A). Second, an LfD algorithm that can be easily used to encode the demonstrated trajectory data is preferable. We elect to utilize Gaussian Mixture Model (GMM) and Gaussian Mixture

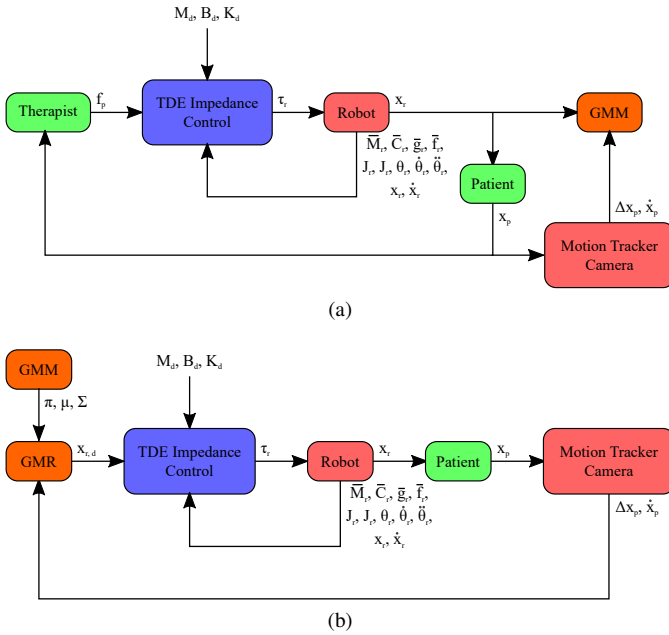


Fig. 1. High-level block diagrams of data flow and interaction between different agents (i.e., the therapist, patient, robot, and motion tracker camera). (a) shows the process flow when the therapist and patient interact to provide training demonstrations and (b) shows the process flow when the patient is practicing alone with assistance from the robot.

Regression (GMR) based techniques (explained in Section II-B). An overview of the system is provided in Fig. 1.

### A. Impedance Control for PHRI

An impedance control scheme is selected to allow the therapist and patient to safely interact with the robot. Impedance controllers produce a desired force based on a predefined relationship with the robot's motion, often described in terms of mechanical inertia, damping, and stiffness. Since our task involves lifting a potentially substantial portion of the patient's body weight, a more heavy-duty robot than those typically seen in rehabilitation robotics is required. However, internal gearing in the joints of such robots produces an apparent inertia of  $n^2 I$ ,  $n$  representing the gear ratio, meaning the robot is typically impossible to move passively. The use of impedance control addresses this issue for larger geared robots, making it easy for a user to move the controlled robot. Note that an admittance controller, an alternative force control method that produces a desired motion depending on force input, could have been employed [26]. However, admittance controllers typically present instability when in contact with environments with high impedances, such as a human gripping and holding a robot in place. On the other hand, impedance control is ideal for maintaining safety in robotic control under environmental contact (e.g., during PHRI), but requires the dynamics of the robot to be well modelled [31]. In our scenario, the robot dynamics can be written as

$$M_r(\theta_s) \ddot{\theta}_r + C_r(\theta_r, \dot{\theta}_r) \dot{\theta}_r + g_r(\theta) + f_r(\theta_r, \dot{\theta}_r) - J_r f_p = \tau_r \quad (1)$$

where  $\theta_r$  represents the robot joint angles,  $M_r$  the moment of inertia matrix,  $C_r$  the Coriolis and centrifugal matrix,  $g_r$  the gravity vector,  $J_r$  the robot's Jacobian,  $f_r$  the robot's joint friction vector,  $f_p$  the force exerted by the patient on the robot end-effector, and  $\tau_r$  the controller motor torque. Please note that the dependence on  $\theta_r$  will be dropped for brevity. The non-linear terms  $M_r$ ,  $C_r$ ,  $g_r$  and  $f_r$  can be roughly modelled, but will likely be inaccurate leading to potentially undesired dynamics.

The Time Delay Estimation (TDE) method, as presented in [32], [33], is used here to reduce the inaccuracy when estimating these non-linear terms. Our approximate model gives us the nominal values  $\{\bar{M}_r, \bar{C}_r, \bar{g}_r, \bar{f}_r\}$ . We can then rewrite (1) as

$$\bar{M}_r \ddot{\theta}_r + (M_r - \bar{M}_r) \ddot{\theta}_r + \dots + \bar{f}_r + (f_r - \bar{f}_r) - J_r f_p = \tau_r \quad (2)$$

which separates the nominal dynamics values from the unknown model errors for each non-linear term. The uncertain non-linear terms can then be grouped together:

$$N = (M_r - \bar{M}_r) \ddot{\theta}_r + \dots + (f_r - \bar{f}_r) \quad (3)$$

The TDE method approximates the non-linear terms  $N$  at a time  $t$ , e.g.,  $N(t)$ , by equating them to the previously measured torque values at a time  $t - T$ , provided  $T$  is small:

$$N(t) \approx N(t - T) = \tilde{N} = \tilde{\tau}_r + \tilde{J}_r \tilde{f}_p - \tilde{M}_r \tilde{\theta}_r - \dots - \tilde{f}_r \quad (4)$$

where the tilde symbol indicates time delay measured values. The desired impedance dynamics are given as

$$M_d(\ddot{x}_r - \ddot{x}_{r,d}) + B_d(\dot{x}_r - \dot{x}_{r,d}) + K_d(x_r - x_{r,d}) = f_d \quad (5)$$

where  $M_d$ ,  $B_d$ , and  $K_d$  represent the desired mass, damping, and stiffness impedance parameters,  $x_r$  represents the robot's Cartesian end-effector position, and  $f_d$  represents the desired output force. By equating  $f_d$  to  $f_p$  and using the relationship between Cartesian and joint space acceleration

$$\ddot{x}_r = J_r \ddot{\theta}_r + \dot{J}_r \dot{\theta}_r \quad (6)$$

we can combine (2), (4), and (5) in order to express the desired robot joint torque controller as

$$\tau_r = \bar{M}_r J_r^{-1} \left\{ \ddot{x}_{r,d} - M_d^{-1} [B_d(\dot{x}_r - \dot{x}_{r,d}) + K_d(x_r - x_{r,d}) - f_p] - \dot{J}_r \dot{\theta}_r \right\} + \bar{C}_r \dot{\theta}_r + \bar{g}_r + \bar{f}_r + \tilde{N} - J_r f_p \quad (7)$$

which effectively provides interactions in Cartesian space. For more details on this process, readers are encouraged to see [32].

### B. Gaussian Mixture Model and Regression

As stated, the basis of the LfD paradigm lies in the incorporation of two phases: the demonstration phase, where the robot observes and statistically encodes trajectories that are physically demonstrated to it, and the imitation phase, where the robot performs regression on the model generated in the demonstration phase. The choice of algorithm for the trajectory encoding is a widely researched topic.

We choose to incorporate a GMM based approach for our learning algorithm. GMMs are probability density functions used to cluster data, constructed as weighted sums of Gaussian component densities [34]. GMMs are well suited to learning human and robot movements in the context of rehabilitation medicine. Their generative modeling properties allow them to smoothly interpolate between the captured underlying aspects of a demonstrated movement as opposed to assigning strict decision boundaries between different phases of a movement. This is especially important for the gait therapy application we present, where gait patterns can vary from trial to trial even for a single user. GMMs also require relatively small training datasets as compared to other machine learning methods such as neural networks and deep learning methods.

The formulaic expression for a GMM is given as

$$p(\xi) = \sum_{k=1}^{N_k} p(k) p(\xi|k) \quad (8)$$

with a total of  $N_k$  Gaussian components in the model,  $p(k)$  being the priors,  $p(\xi|k)$  being the conditional density functions, and  $\xi$  being a  $D$ -dimensional data vector containing both the input and output variables needed during regression.  $p(k)$  and  $p(\xi|k)$  are computed as functions of the model variables  $\{\pi_k, \mu_k, \Sigma_k\}$ , which represent the prior probabilities, mean vectors, and covariance matrices that define each Gaussian component. Further details can be found in [34]. In our experiments, we opt for a simpler characterization of the patient's gait cycle than what is typically seen in other gait therapy works; we record only the difference in the toe positions of each foot and the velocity of the unimpaired foot, as opposed to the joint rotations of the full leg. The data vector is then given by  $\xi = [\Delta x_p, \dot{x}_{p,u}, x_r]^T$ , with  $\Delta x_p$  representing the difference in patient foot position (e.g.,  $\Delta x_p = x_{p,right} - x_{p,left}$ ),  $\dot{x}_{p,u}$  representing the patient's unaffected foot's velocity, and  $x_r$  representing the robot's end-effector position.

We then incorporate GMR during the imitation phase in order to extract the desired therapeutic behavior of the robot from our learned model. GMR leverages the Gaussian conditioning theorem and linear combination properties of Gaussian distributions to retrieve the mean output values ( $\hat{\xi}_s$ ), referred to as the conditional expectation, from a GMM, as well as the variances in those values, referred to as the conditional covariance ( $\hat{\Sigma}_s$ ). Again, further details can be found in [34].

Fig. 2 depicts the LfD procedure as described.

### III. EVALUATION

#### A. Experimental Setup

We evaluated the system with a standard locomotion task, where 2 able-bodied study participants (male, 23 years old, and male, 24 years old) walked on a manually powered treadmill. They wore an elastic cord attached between their heel and calf that emulated foot drop during locomotion. The elastic cord is stiff enough to ensure the toe fully drops during a step. A ClaroNav MicronTracker (ClaroNav, Inc., Toronto, Ontario, Canada) motion tracking camera was used to record the positions of both of the patient's feet. The participant

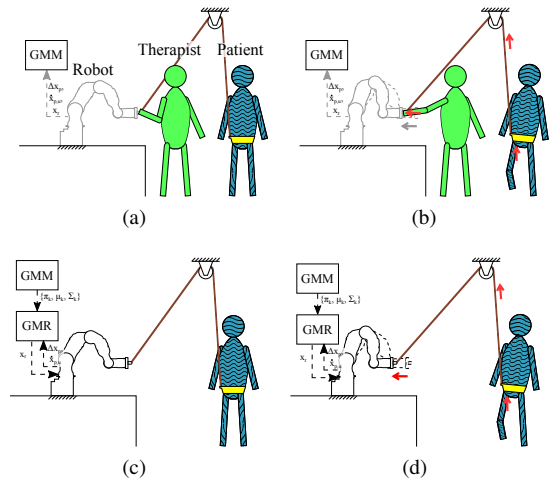


Fig. 2. A generalized diagram of the LfD procedure employed in this work. In (a), the therapist and participant cooperatively interact while completing the walking task, with the therapist providing assistance by moving the robot as shown in (b). The learning system then learns the therapist's behavior from the provided demonstrations in phases (a) and (b), characterized as desired positions for the robot. Then, in diagrams (c) and (d), the robot replicates the learned behavior, allowing the participant to practice the gait therapy task in the therapist's absence while experiencing the therapist's assistance.

wore a waist-level harness attached to a rehab robot by a rope and pulley system. The hip is chosen as the attachment site for simplicity, as it moves the least in the horizontal plane during gait. A Motoman SIA-5F (Yaskawa America, Inc., Miamisburg, Ohio, USA) seven Degrees-of-Freedom (DoF) serial manipulator was used as the rehab robot, with a 6-DoF ATI Gamma Net force and torque sensor (ATI Industrial Automation, Inc., Apex, North Carolina, USA) attached at the robot's wrist joint before the end-effector. The robot was simplified to a 2-DoF RR planar robot, which moved in 1-DoF that the waist harness was hoisted linearly upwards by the pulley. The therapist was represented by a third able-bodied individual (Fig. 3). 2 additional participants were also tested, but due to the poor quality of their motion tracker data, these results were not included.

The impedance parameters in (5) were chosen experimentally. For demonstrations,  $M_d$  and  $K_d$  were given values permissive to free movement, while the damping parameter  $B_d$  was given a higher value and decreased until instability was observed. For imitations,  $K_d$  was adjusted to instead provide accurate trajectory tracking. Final values for the parameters were given as  $M_d = 4.94 \text{ N}\cdot\text{s}^2/\text{m}$ ,  $B_d = 80.52 \text{ N}\cdot\text{s}/\text{m}$ , and  $K_d = 0$  for demonstrations. For imitations,  $M_d$  and  $B_d$  were unchanged and  $K_d = 311.29 \text{ N}/\text{m}$ , around a third of a value based on a previous study on measuring the impedance of a stiff upper arm (911.29 N/m) performed by our group. Desired accelerations and velocities were zero at all times, and desired positions were provided by regression during imitation. Estimates of the robot dynamics model nominal parameters  $\bar{M}_r$  and  $\bar{C}_r$  in (2) were performed as in [35] for a 2-DoF robot, while  $\bar{g}_r$  and  $\bar{f}_r$  are estimated to be negligible ( $\bar{g}_r = 0$  as the robot is positioned in a gravity neutral orientation, i.e., where the joints of the robot that are controlled by the impedance controller are oriented to rotate in the horizontal plane only and

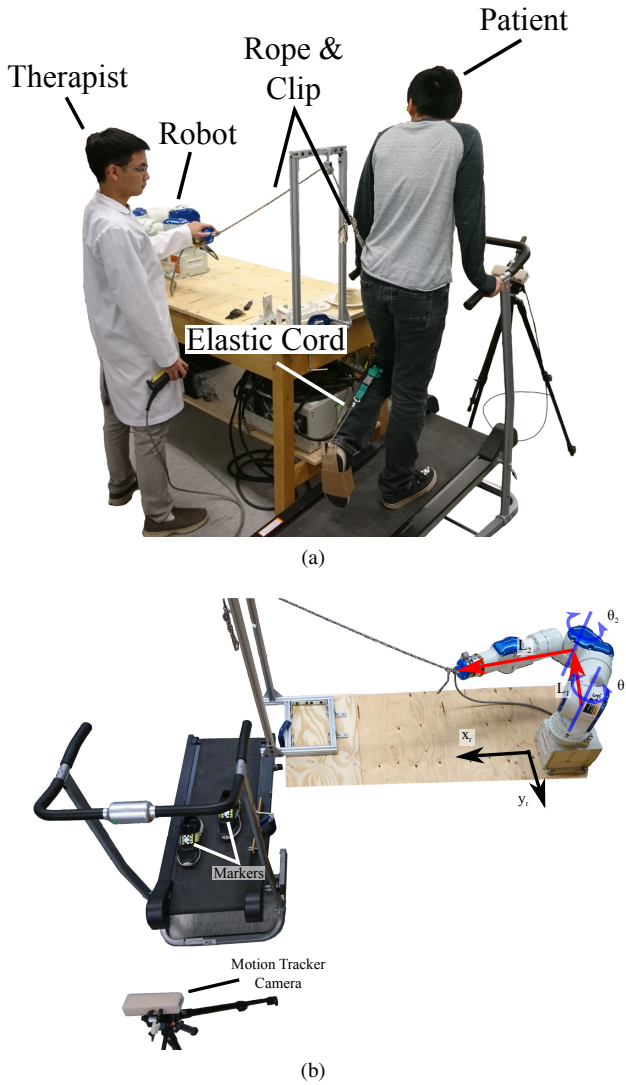


Fig. 3. Experiment setup. In (a) the robot is moved by the therapist by holding and pressing on its end-effector force sensor. This provides a lifting assistance to the patient who walks at their selected pace on the treadmill while harnessed to the robot through the rope and clip. During both the demonstration and imitation phases, the patient, played by a healthy participant, wears the elastic cord in order to simulate foot drop. In (b) the motion tracker camera is shown placed in front of the patient so as to capture the positions of their toes, which are registered to markers placed on the tops of their shoes. The simplified 2-DoF kinematics of the robot are also shown.

are thereby not under the effects of gravity). The remaining joints of the robot were held static with a PID controller.

## B. Results

Five demonstrations were first performed to train the system. While wearing the elastic cord on the left foot (representing the limb with foot drop), the participant was assisted by the therapist and completed 10 gait cycles per demonstration. A GMM of 9 components ( $N_k = 12$ ) was generated from these demonstrations. This selection was partially motivated by considering the common interpretation of the gait cycle as having 8 phases; model generation was therefore tested for 8 or more components. Using the generated model, five imitations were recorded in which the participant completed the same gait task wearing the elastic cord but with the assistance of

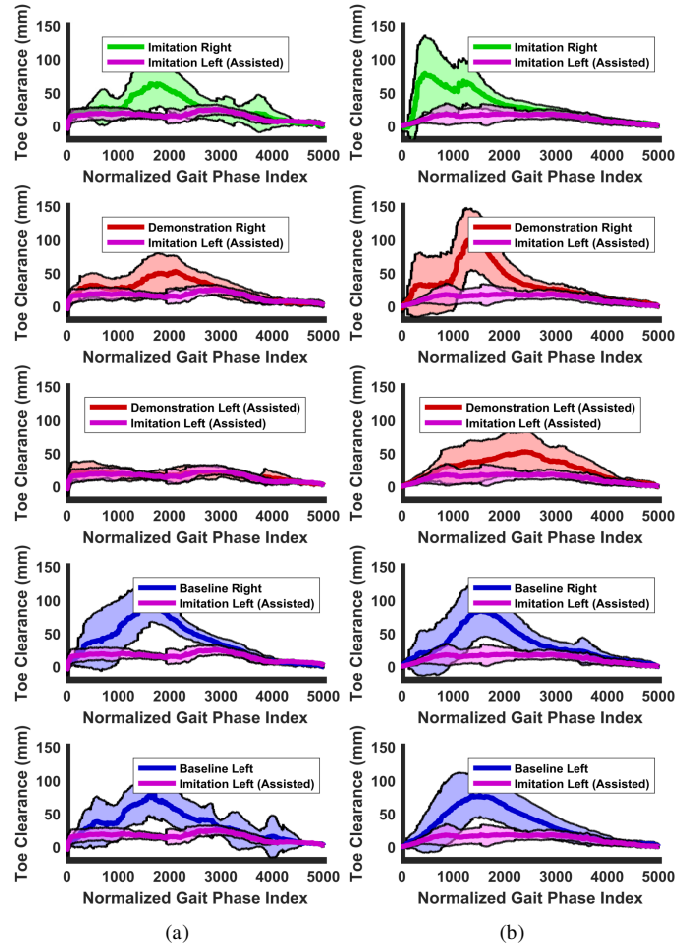


Fig. 4. Comparison of toe clearance between the assisted left foot during imitation and each of the left and right feet in the other scenarios. Results for Participant 1 are shown in (a) and Participant 2 in (b). Mean values are represented by the solid colored lines, while one standard deviation is shown by the filled area around each trajectory. All trajectories are normalized to 5000 data points using spline interpolation, allowing for later comparison with the Kolmogorov-Smirnov test.

the robot instead of the therapist. An additional five baseline datasets were recorded without therapist or robot intervention and without the elastic cord as a handicap, providing baseline data of an able-bodied individual for comparison later. These three sets of data are referred to as the “demonstration”, “imitation”, and “baseline” datasets or scenarios from hereon.

Motion tracker data of each foot and the treadmill surface were used to generate the toe clearance values for the assisted and normal datasets during the gait cycle for each foot. The trajectories were normalized to 5000 samples each to provide consistency in comparison, where the swing phase is found in the first portion of the data and the stance phase in the second (Fig. 4). The averages of the maximum toe clearances for each foot in each of the scenarios were also found (Table D).

As we also aimed to examine the similarity between the toe clearance trajectories, the Kolmogorov-Smirnov hypothesis test was performed between the imitation (assisted) left foot dataset (representing the foot with foot drop) and each of the other datasets. The toe clearances of each scenarios’ gait cycles at each normalized index of the trajectory were treated as

TABLE I  
MEAN AND STANDARD DEVIATION VALUES OF MAXIMUM TOE CLEARANCES.

	Participant 1					
	Imitation		Demonstration		Baseline	
	Right	Left	Right	Left	Right	Left
Mean (mm)	92.65	33.26	78.44	39.12	113.71	106.90
SD (mm)	24.68	9.58	21.19	11.69	23.28	21.25
	Participant 2					
	Imitation		Demonstration		Baseline	
	Right	Left	Right	Left	Right	Left
Mean (mm)	127.97	32.44	140.19	82.36	131.72	118.74
SD (mm)	25.38	13.11	31.09	32.40	22.51	32.38

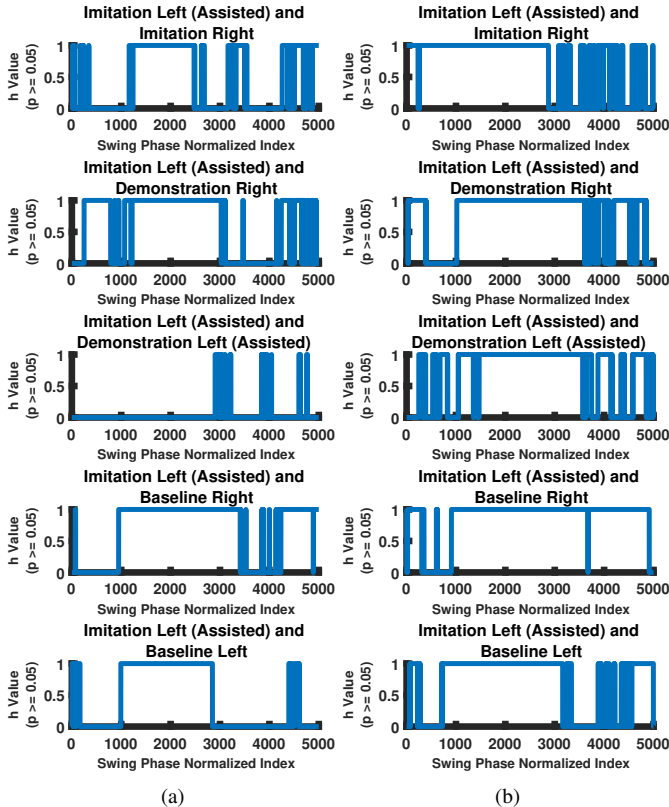


Fig. 5. Kolmogorov-Smirnov test performed for each normalized index. The diagrams depict the statistical similarities between the imitation (assisted) left foot’s trajectories and each of the other scenarios. Results for Participant 1 are shown in (a) and Participant 2 in (b). The hypothesis measure ( $h$ ) represents whether the two are statistically similar:  $h = 0$  represents the null hypothesis (i.e., the signals are statistically similar at the point of comparison) and  $h = 1$  represents statistical dissimilarity. The imitation (assisted) left foot achieves similar clearance values only much earlier in its swing phase to the other datasets, with the exception of Participant 1’s demonstration scenario left foot measurements with which it matches throughout the entire cycle.

individual distributions, across which the test was performed (Fig. 5).

#### IV. DISCUSSION

From Fig. 4 we see that the system would indeed be able to assist a patient with foot drop to achieve toe clearance (specifically the imitation (assisted) left foot), and in turn practice gait therapy on his/her own. No sudden, unsafe or unstable movements were experienced, showing that the proper interaction was learned and that the impedance controller

functions adequately for the task. However, we see that even at each foot’s maximum clearance (Table I), the assisted left foot during imitation ( $33.26 \pm 9.58$  mm for Participant 1,  $32.44 \pm 13.11$  mm for Participant 2) does not rise within a standard deviation of any of the other trajectories except for the demonstration (assisted) left foot for Participant 1 ( $39.12 \pm 11.69$  mm), motivating further examination of the similarity of the robot-assisted left foot trajectory to the others. The Kolmogorov-Smirnov results confirm this observed dissimilarity; the null hypothesis ( $h = 0, p > 0.05$ ), stating that the trajectories are statistically similar, is only confirmed for sparse segments of the gait cycle, nearer to the beginning of the other trajectories.

A qualitative examination of the toe clearance trajectories provides some insight into possible reasons behind these observations. The trajectories other than for the imitation and demonstration (assisted) left foot datasets distinctly peak around halfway through the swing phase (50% – 60% of the swing phase). Both assisted left foot datasets, on the other hand, peak very late in the phase (80% of the swing phase). This phase shift could be attributed to a number of factors. First, it is highly plausible that the demonstration data provided by the therapist’s assistance was timed incorrectly, and their intervention was phase shifted with respect to the participant’s walking pattern; this is evident in the visual similarities between the demonstration and imitation data for the (assisted) left foot. A second cause could likely have been the stiffness of the robot during the imitation phase was too low ( $K_d = 311.29N/m$ ). Another possible reason could be that the intermittently applied change in the participant’s center of gravity negatively affected his/her gait pattern, leading to a period in the cycle (20% – 50% of the swing phase) where the participant resisted the robotic assistance until comfortable. Lastly, the generative properties of GMMs tend to pull the model’s components away from curves in trajectories, leading to an observable “corner cutting” effect. When using GMR with the produced model, the desired output could then effectively have a damped behavior as compared to what was demonstrated. These same factors could also produce the reduced maximum toe clearances observed as well. One important caveat is that only toe clearance values were recorded. With the simulated foot drop, the toe is the lowest point of the foot during the swing phase; however, in normal gait, the heel is lowest when preparing for heel strike. It could be beneficial to record the positions of the heel as well, but this would require a more advanced motion capture system to capture the motion from behind the patient.

We suggest a number of possible improvements that could address these shortcomings. First and foremost would be to have experienced, actual rehabilitation practitioners perform the role of the therapist, as their expertise would likely produce improved results in the tracking of an appropriate gait pattern. In addition to this, results could also be improved if the compliance of the robot during the demonstration phase was increased. The impedance controller is fundamentally limited by the design of the robot; compliance was increased as much as possible through lowering the terms  $M_d$ ,  $B_d$ , and  $K_d$ , but  $M_d$  is lower bounded by the physical mass of the robot and

$B_d$  was required to be non-zero for stability. As a result, moving the robot required the therapist to exert as much force as the body weight percentage they were supporting, on top of the mass and damping the robot presented which could result in less accurate movements. An adaptive impedance control system could be a possible solution, where depending on some measure of sensed therapist intention the robot relaxes or increases its impedance parameters. With regards to the stiffness of the robot during the imitation phase, it may help to increase the value or to also implement an adaptive controller. The value was chosen by using one-third of a value for a stiff arm found in an earlier work by our group, in order to allow for safe and gentle guidance. However, it is likely that the system was too forgiving and thus had difficulty actually lifting the participant properly as is most clearly seen in Participant 2's left foot imitation results not resembling their left foot demonstration results. It would be beneficial to perform a future study focused on how to properly tune the impedance parameters or to implement an adaptive parameter tuning system. With regards to the learning algorithm, modifying Gaussian-based modeling methods to place more emphasis on curves in trajectories, as in [36], could help to address the hypothesized issues arising from the generative nature of the models. Lastly, increasing the participant population would benefit the study tremendously. Having more participants with a wider variation in gait patterns, as well as actual symptomatic patients would provide results more likely to be applicable to the intended population.

## V. CONCLUSION

In this paper, impedance control based teaching of a robot was used to teach a therapist's assistance to a robot during a treadmill-based therapy routine for a participant with foot drop. GMM and GMR were used as the learning and regression algorithms needed to train the robot and have it imitate the therapist later. We show the system is able to successfully provide toe clearance during gait, although the imitation is not quite able to produce clearance values comparable to normal gait. Future work will focus on improving the learning algorithm to account for these inaccuracies, better tuning the impedance controller, and eventually testing the system with more participants and in clinical settings.

## REFERENCES

- [1] R. Voelker, "Rehabilitation medicine welcomes a robotic revolution," *JAMA*, vol. 294, no. 10, pp. 1191–1195, 2005.
- [2] E. J. Benjamin *et al.*, "Heart disease and stroke statistics—2017 update: A report from the american heart association," *Circulation*, 2017.
- [3] P. Lum *et al.*, "Robotic devices for movement therapy after stroke: Current status and challenges to clinical acceptance," *Topics in Stroke Rehabilitation*, vol. 8, no. 4, pp. 40–53, 2002. PMID: 14523729.
- [4] C. M. Sackley, "The relationships between weight-bearing asymmetry after stroke, motor function and activities of daily living," *Physiotherapy Theory and Practice*, vol. 6, no. 4, pp. 179–185, 1990.
- [5] A. P. Yelnik *et al.*, "Perception of verticality after recent cerebral hemispheric stroke," *Stroke*, 2002.
- [6] M. R. Schindl *et al.*, "Treadmill training with partial body weight support in nonambulatory patients with cerebral palsy," *Archives of Physical Medicine and Rehabilitation*, vol. 81, no. 3, pp. 301 – 306, 2000.
- [7] K.-H. Mauritz, "Gait training in hemiplegia," *European Journal of Neurology*, vol. 9, no. s1, pp. 23–29.
- [8] N. E. Mayo *et al.*, "A new approach to retrain gait in stroke patients through body weight support and treadmill stimulation," *Stroke*, 1998.
- [9] C. Werner *et al.*, "Treadmill training with partial body weight support and an electromechanical gait trainer for restoration of gait in subacute stroke patients," *Stroke*, 2002.
- [10] S. Hussain, S. Q. Xie, and G. Liu, "Robot assisted treadmill training: Mechanisms and training strategies," *Medical Engineering & Physics*, vol. 33, no. 5, pp. 527 – 533, 2011.
- [11] I. Díaz, J. J. Gil, and E. Sánchez, "Lower-limb robotic rehabilitation: literature review and challenges," *Journal of Robotics*, vol. 2011, 2011.
- [12] W. Meng *et al.*, "Recent development of mechanisms and control strategies for robot-assisted lower limb rehabilitation," *Mechatronics*, vol. 31, pp. 132 – 145, 2015.
- [13] S. Jezernik *et al.*, "Adaptive robotic rehabilitation of locomotion: a clinical study in spinally injured individuals," *Spinal Cord*, vol. 41, no. 12, p. 657, 2003.
- [14] J. Cao *et al.*, "Control strategies for effective robot assisted gait rehabilitation: The state of art and future prospects," *Medical Engineering & Physics*, vol. 36, no. 12, pp. 1555 – 1566, 2014.
- [15] R. Garate *et al.*, "Experimental validation of motor primitive-based control for leg exoskeletons during continuous multi-locomotion tasks," *Frontiers in Neurobotics*, vol. 11, p. 15, 2017.
- [16] K. Gui, H. Liu, and D. Zhang, "Toward multimodal human–robot interaction to enhance active participation of users in gait rehabilitation," *IEEE Transactions on Neural Systems and Rehabilitation Engineering*, vol. 25, no. 11, pp. 2054–2066, 2017.
- [17] M. F. Eilenberg, H. Geyer, and H. Herr, "Control of a powered ankle-foot prosthesis based on a neuromuscular model," *IEEE Transactions on Neural Systems and Rehabilitation Engineering*, vol. 18, no. 2, pp. 164–173, 2010.
- [18] A. R. Wu *et al.*, "An adaptive neuromuscular controller for assistive lower-limb exoskeletons: A preliminary study on subjects with spinal cord injury," *Frontiers in Neurobotics*, vol. 11, p. 30, 2017.
- [19] H. Vallery *et al.*, "Reference trajectory generation for rehabilitation robots: complementary limb motion estimation," *IEEE Transactions on Neural Systems and Rehabilitation Engineering*, vol. 17, no. 1, pp. 23–30, 2009.
- [20] V. Rajasekaran, J. Aranda, and A. Casals, "Adaptive walking assistance based on human-orthosis interaction," in *Intelligent Robots and Systems (IROS), 2015 IEEE/RSJ International Conference on*, pp. 6190–6195, IEEE, 2015.
- [21] J. A. Blaya and H. Herr, "Adaptive control of a variable-impedance ankle-foot orthosis to assist drop-foot gait," *IEEE Transactions on Neural Systems and Rehabilitation Engineering*, vol. 12, no. 1, pp. 24–31, 2004.
- [22] C. C. Chen and R. K. Bode, "Factors influencing therapists' decision-making in the acceptance of new technology devices in stroke rehabilitation," *American journal of physical medicine & rehabilitation*, vol. 90, no. 5, pp. 415–425, 2011.
- [23] M. Maaref *et al.*, "A gaussian mixture framework for co-operative rehabilitation therapy in assistive impedance-based tasks," *IEEE Journal of Selected Topics in Signal Processing*, vol. 10, pp. 904–913, Aug 2016.
- [24] C. Martínez and M. Tavakoli, "Learning and robotic imitation of therapist's motion and force for post-disability rehabilitation," in *Systems, Man, and Cybernetics (SMC), 2017 IEEE International Conference on*, pp. 2225–2230, IEEE, 2017.
- [25] M. Najafi *et al.*, "Robotic assistance for children with cerebral palsy based on learning from tele-cooperative demonstration," 01 2017.
- [26] J. Fong and M. Tavakoli, "Kinesthetic teaching of a therapist's behavior to a rehabilitation robot," in *2018 International Symposium on Medical Robotics (ISMR)*, pp. 1–6, March 2018.
- [27] R. Begg and J. Kamruzzaman, "A machine learning approach for automated recognition of movement patterns using basic, kinetic and kinematic gait data," *Journal of Biomechanics*, vol. 38, no. 3, pp. 401 – 408, 2005.
- [28] M. Hansen *et al.*, "Real time foot drop correction using machine learning and natural sensors," *Neuromodulation: Technology at the Neural Interface*, vol. 5, no. 1, pp. 41–53.
- [29] M. Peshkin *et al.*, "Kineassist: a robotic overground gait and balance training device," in *9th International Conference on Rehabilitation Robotics, 2005. ICORR 2005.*, pp. 241–246, June 2005.
- [30] J. D. Stewart, "Foot drop: where, why and what to do?," *Practical Neurology*, vol. 8, no. 3, pp. 158–169, 2008.
- [31] N. Hogan and S. P. Buerger, "Impedance and interaction control," in *Robotics and automation handbook* (T. R. Kurfess, ed.), ch. 19, CRC press, 2004.

- [32] J. W. Jeong, P. H. Chang, and K. B. Park, "Sensorless and modeless estimation of external force using time delay estimation: application to impedance control," *Journal of mechanical science and technology*, vol. 25, no. 8, p. 2051, 2011.
- [33] R. Tao, *Haptic teleoperation based rehabilitation systems for task-oriented therapy*. PhD thesis, University of Alberta, 2014.
- [34] S. Calinon, *Robot Programming by Demonstration: A Probabilistic Approach*. EPFL/CRC Press, 2009. EPFL Press ISBN 978-2-940222-31-5, CRC Press ISBN 978-1-4398-0867-2.
- [35] M. W. Spong and M. Vidyasagar, *Robot dynamics and control*. John Wiley & Sons, 2008.
- [36] C. Lauretti *et al.*, "Learning by demonstration for planning activities of daily living in rehabilitation and assistive robotics," *IEEE Robotics and Automation Letters*, vol. 2, pp. 1375–1382, July 2017.